5236 *Biochemistry* **2010,** *49,* 5236–5243
DOI: 10.1021/bi1001322

BIOCHEMISTRY
including biophysical chemistry & molecular biology
Article

Mapping of Lysine Methylation and Acetylation in Core Histones of *Neurospora crassa*[†]

Lei Xiong,[‡] Keyur K. Adhvaryu,[§] Eric U. Selker,[§] and Yinsheng Wang*[,‡]

[‡]*Department of Chemistry, University of California, Riverside, California 92521-0403, and* [§]*Institute of Molecular Biology, University of Oregon, Eugene, Oregon 97403*

Received January 27, 2010; Revised Manuscript Received April 26, 2010

ABSTRACT: Core histones are susceptible to a variety of post-translational modifications (PTMs), among which methylation and acetylation play critical roles in various chromatin-dependent processes. The nature and biological functions of these PTMs have been extensively studied in plants, animals, and yeasts. In contrast, the histone modifications in *Neurospora crassa*, a convenient model organism for multicellular eukaryotes, remained largely undefined. In this study, we used several mass spectrometric techniques, coupled with HPLC separation and multiple-protease digestion, to identify the methylation and acetylation sites in core histones isolated from *Neurospora*. Electron transfer dissociation (ETD) was employed to fragment the heavily modified long N-terminal peptides. In addition, accurate mass measurement of fragment ions allowed for unambiguous differentiation of acetylation from trimethylation. Many modification sites conserved in other organisms were identified in *Neurospora*. In addition, some unique modification sites in histone H2B, including N-terminal α methylation, methylation at K3, and acetylation at K19, K28, and K29, were observed. Our analysis provides a potentially comprehensive picture of methylation and acetylation of core histones in *Neurospora*, which should serve as a foundation for future studies of the function of histone PTMs in this model organism.

The eukaryotic nucleosome, the fundamental unit of chromatin, plays an important role in packaging and organizing the genetic material (*1*). Each nucleosome consists of 146 bp of DNA wrapped around an octameric core histone complex consisting of two H2A−H2B dimers flanking a $(H3-H4)_2$ tetramer (*1*, *2*). All core histones have a basic N-terminal domain, a globular domain organized by the histone fold, and a C-terminal tail (*1*, *2*). The histone N-terminal tails, which extend out from the core particle, are involved in the establishment of chromatin structural states, whereas their histone fold domains mediate histone−histone and histone−DNA interactions (*2*).

Core histones are susceptible to a variety of post-translational modifications (PTMs),[1] which include methylation, acetylation, phosphorylation, ubiquitination, SUMOylation, and ADP ribosylation. These modifications, which occur mainly on the N-terminal tails (*3*, *4*), can affect interactions of nucleosomes with trans-acting factors and are thought to play a role in the assembly and disassembly of chromatin states and can control the accessibility of DNA for important cellular processes, including transcription, replication, gene silencing, and DNA repair (*5*−*9*). Distinct modifications of the histone tails can recruit specific chromatin-binding proteins, and modifications on the same or different histone tails may be interdependent and generate various combinations on any individual nucleosome (*10*−*12*).

Mass spectrometry has been widely used for assessing histone PTMs. It provides direct information about the sites and types of modifications, differentiates isobaric modifications (e.g., acetylation vs trimethylation) (*13*), and allows for quantitative analysis (*14*). PTM information obtained by mass spectrometric analysis facilitates genome-wide functional studies and provides the foundation for studies of modifications in specific regions of genomes using chromatin immunoprecipitation (ChIP) with antibodies recognizing specifically modified histones (*15*−*17*).

Neurospora crassa is a convenient model eukaryote, showing genomic features lacking in some other simple eukaryotes (e.g., yeast), including DNA methylation and certain histone modifications (e.g., H3K27 methylation). Studies using this organism have contributed significantly to the fundamental understanding of circadian rhythms, DNA methylation, genome defense systems, mitochondrial protein import, post-transcriptional gene silencing, DNA repair, and other processes (*18*). Being a multicellular filamentous fungus, *Neurospora* also provides a system for studying cellular differentiation and development (*19*). However, no comprehensive investigation of the PTMs of *Neurospora* core histones has been reported.

In this study, we extracted core histones from *N. crassa* and systematically mapped histone methylation and acetylation, using a combination of digestion with various proteases and analyses with multiple types of mass spectrometers. Our results allowed for the identification of acetylation and methylation sites of lysine residues that were found previously in *Arabidopsis thaliana*, *Saccharomyces cerevisiae*, and humans. More importantly, we identified several unique acetylation and methylation sites in core histones of *Neurospora*. Our analysis of core histone PTMs provides a foundation for examining the regulation of histone modifications and for genome-wide functional studies in this model organism.

EXPERIMENTAL PROCEDURES

Extraction of Core Histones from N. crassa. N. crassa was cultured as described previously (*20*−*22*) and stored at −80 °C.

[†]This work was supported by National Institutes of Health Grants GM068087, CA116522, and GM025690.

*To whom correspondence should be addressed. E-mail: yinsheng.wang@ucr.edu. Telephone: (951) 827-2700. Fax: (951) 827-4713.

[1]Abbreviations: PTM, post-translational modification; ETD, electron transfer dissociation; ChIP, chromatin immunoprecipitation; CID, collisionally induced dissociation.

 Published on Web 04/30/2010

The core histones were obtained by using procedures reported for the isolation of nuclei by Emmett et al. (*23*) and histone extraction by Goff (*24*) with some modifications. Briefly, frozen *Neurospora* tissue (5 g) was ground to a fine powder with a pestle in a cold mortar under liquid nitrogen. To the powder was subsequently added 20 mL of nucleus isolation buffer containing 0.3 M sucrose, 40 mM $HaHSO_3$, 25 mM Tris-HCl (pH 7.4), 10 mM $MgSO_4$, 0.5 mM EDTA, and 0.5% NP40, and the suspension was stirred vigorously. Cells were disrupted by intermittent exposure of the homogenate to sonication. The resulting mixture was filtered through two layers of silk in a Büchner funnel to remove whole cells and cell debris.

The filtrate described above was centrifuged at 7500*g* for 10 min, and the supernatant was removed. To the precipitate was subsequently added 50 mL of nucleus isolation buffer, and the resulting mixture was gently shaken for 30 min and centrifuged again. The precipitate, which contained the nuclei, was resuspended in 1 mL of ice-cold $NaHSO_3$ solution (25 mM, pH 7.2), followed by brief sonication (5 s). Hydrochloric acid was added immediately to the suspension to a final concentration of 0.3 M, and the resulting mixture was incubated at 4 °C for 1 h with continuous vortexing on an automatic vortexing machine. The histones in the supernatant were precipitated with cold acetone, centrifuged, dried, and redissolved in water.

High-Performance Liquid Chromatography (HPLC) Separation and Protease Digestion. Core histones were isolated by HPLC on an Agilent 1100 system (Agilent Technologies, Santa Clara, CA) as described previously (*25*). A 4.6 mm × 250 mm C4 column (Grace Vydac, Hesperia, CA) was used. The wavelength for the UV detector was 220 nm. The flow rate was 0.8 mL/min, and a 60 min linear gradient from 30 to 60% acetonitrile in 0.1% trifluoroacetic acid (TFA) was employed.

To obtain high sequence coverage of the proteins, purified histones were digested separately with several proteases, including trypsin, Arg-C, Glu-C, Asp-N, and chymotrypsin. A protein:enzyme ratio of 50:1 (w/w) was employed for trypsin and 20:1 for other proteases. The different buffers used for the digestions were 100 mM NH_4HCO_3 (pH 8.0) for trypsin, Arg-C, or Glu-C; 50 mM sodium phosphate (pH 8.0) for Asp-N; and 100 mM Tris-HCl (pH 7.8) along with 10 mM $CaCl_2$ for chymotrypsin. The digestion was conducted overnight at room temperature for chymotrypsin and at 37 °C for other proteases. The peptide mixtures were subjected directly to LC−MS/MS analysis, or to a further peptide fractionation by HPLC and then analyzed by MALDI-MS/MS on a Q-STAR instrument or ESI-MS/MS on an LTQ-Orbitrap (see below).

Peptide fractionation was performed on the same HPLC system with a Zorbax SB-C18 capillary column (0.5 mm × 150 mm, 5 μm particle size, Agilent Technologies), and a 60 min gradient from 2 to 60% acetonitrile in 0.6% acetic acid was used. The flow rate was 10 μL/min.

Mass Spectrometry. MALDI-MS/MS measurements were performed on a QSTAR XL quadrupole/time-of-flight instrument equipped with an o-MALDI ion source (Applied Biosystems, Foster City, CA). The laboratory collision energy applied for MS/MS varied from 50 to 75 eV depending on peptide sequences and modification levels. The collision gas was nitrogen.

LC−MS/MS experiments were performed on three different instruments, including a 6510 QTOF LC/MS system with an HPLC-Chip Cube MS interface (Agilent Technologies), an LTQ linear ion trap mass spectrometer, and an LTQ-Orbitrap XL mass spectrometer with electron transfer dissociation (ETD) capability (Thermo Electron Co., San Jose, CA). The same 60 min linear gradient from 2 to 60% acetonitrile in 0.1% formic acid was applied for peptide separation.

In the 6510 QTOF LC/MS system, sample enrichment, desalting, and HPLC separation were conducted automatically on the Agilent HPLC-Chip with an integrated trapping column (40 nL) and a separation column (Zorbax 300SB-C18, 75 μm × 150 mm, 5 μm particle size). The Chip spray voltage (VCap) was set at 1950 V and varied depending on chip conditions. MS/MS experiments were conducted in either the data-dependent scan mode or the preselected ion mode. The width for precursor ion selection was 4 *m*/*z* units. The temperature and flow rate for the drying gas were 325 °C and 4 L/min, respectively. Nitrogen was used as the collision gas, and the collision energy followed a linear equation with a slope of 3 V per 100 *m*/*z* units and an offset of 2.5 V. The raw data obtained in the data-dependent scan mode were converted to Mascot generic format files and submitted to the Mascot Database search engine (Matrix Science, Boston, MA) for protein and PTM identification.

For LC−MS/MS analysis on the LTQ, peptides were separated with a Zorbax SB-C18 capillary column (0.5 mm × 150 mm, 5 μm particle size, Agilent Technologies), and the mobile phases were delivered by the Agilent 1100 capillary HPLC pump at a flow rate of 6 μL/min. Helium was employed as the collision gas, and the normalized collision energy was 30%. The spray voltage was 4.5 kV, and the temperature for the ion transport tube was 275 °C.

ETD spectra were recorded on an LTQ-Orbitrap (Thermo Electron Co.). Both on-line LC−MS/MS and off-line direct infusion analyses were performed. In brief, during the on-line LC−MS/MS analysis, samples were redissolved in 15 μL of 0.1% formic acid and loaded on a Biobasic C18 Picofrit capillary column (75 μm × 100 mm, 15 μm particle size, New Objective, Woburn, MA) at a flow rate 0.3 μL/min. The ETD reaction time was 100 ms. In the off-line analysis, the prefractionated H2B and H4 N-terminal peptides were redissolved in 20 μL of a 50:50 acetonitrile/H_2O mixture with 0.1% formic acid. Samples were directly infused. A different ETD reaction time was used to optimize peptide fragmentation.

RESULTS

N. crassa is a convenient model for multicellular eukaryotes, and it has been frequently used for studying the regulation of various cellular processes (*19*). To improve our understanding of chromatin structure and function in *Neurospora*, we initiated a systematic investigation of the PTMs of core histones in this organism. We first extracted core histones from *Neurospora* tissues and fractionated individual core histones by using reverse-phase HPLC. The core histones were eluted in the following order: H2B, H4, H2A, and H3 (Figure S1 of the Supporting Information). We then digested the core histones individually with different proteases and analyzed the peptide mixtures via LC−MS/MS on various instrument platforms to obtain high sequence coverage and achieve unambiguous PTM assignment. The detected PTM sites are summarized in Figure 1, and the sequence coverage is shown in Figure S2 of the Supporting Information.

Identification of PTMs in Histones H2B and H2A. Isolated histone H2B was digested with trypsin, Asp-N, and Glu-C separately, yielding peptides of appropriate length and good sequence coverage. The digestion mixtures were subjected

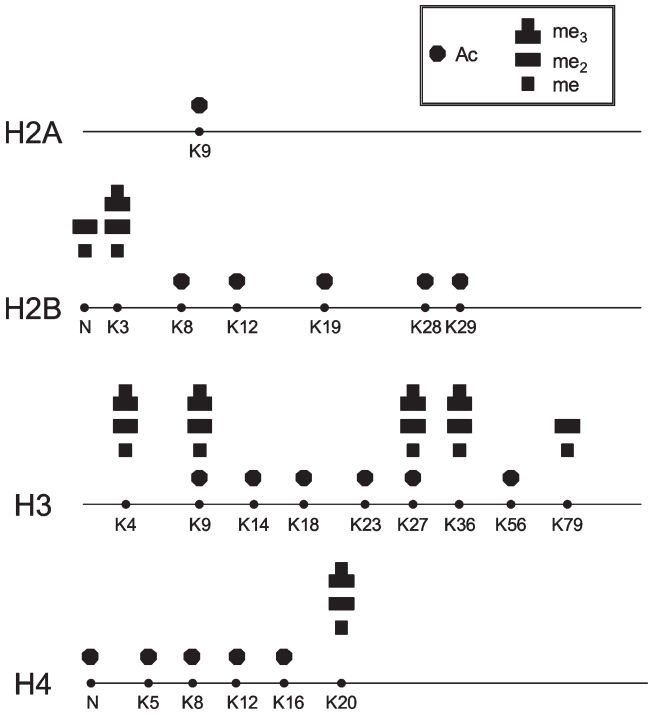

FIGURE 1: Summaries of the detected PTMs of *Neurospora* core histones. The modified residues are labeled, and N represents the N-terminus. Acetylation is designated with solid octagons, and mono-, di-, and trimethylation are represented by one, two, and three square boxes, respectively.

subsequently to LC−MS/MS analysis, and the acquired mass spectra were searched with the Mascot search engine and the results manually verified. A sequence coverage of 100% was reached, and multiple modification sites were identified.

Acetylation of histone H2B was reported for several organisms, including human, budding yeast, and *Arabidopsis* (*26*−*29*). Here we identified many acetylation sites, including K7 and K12, which appear acetylated among different organisms, and K19, K28, and K29, which have not been reported.

Aside from acetylation, we also observed methylation of K3 and of the N-terminus of *Neurospora* H2B. Example mass spectra for the H2B N-terminal peptide $_1$PPKPADKKPASK$_{12}$ are depicted in Figure 2 and Figure S3 of the Supporting Information. Positive-ion ESI-MS (Figure 2A) revealed the presence of one acetyl group and two, three, four, or five methyl groups in this peptide segment. MS/MS of this group of peptides were all recorded with the selected ion monitoring (SIM) mode of analysis. The modification sites could be easily determined from fragment ions, with the consideration of mass shifts introduced by PTMs, e.g., 14.0157 Da for monomethylation and 42.0106 Da for acetylation. MS/MS results revealed that the N-terminus was mono- or dimethylated, K3 was mono-, di-, or trimethylated, and K7 was completely acetylated. In the MS/MS of the dimethylated and monoacetylated peptide (Figure 2B), the existence of the b_6 + 2Me, y_9 + Ac, and y_{11} + Ac + Me ions provides evidence of monomethylation on the N-terminus and K3. We also observed y_4, y_5, and y_6 + Ac ions, providing evidence of acetylation of K7. Similar methylation of an N-terminal proline has been observed in H2B from *Drosophila melanogaster* (*30*) and from gonads of the starfish *Asterias rubens* (*31*). Along this line, N-terminal alanine methylation was found for *Tetrahymena* histone H2B (*32*) and *Arabidopsis* histone H2B variants HTB-9 and HTB-11 (*33*). Moreover, N-terminal α-methylation of the RCC1 protein is believed to promote stable association of RCC1 with chromatin through DNA binding in an α-methylation-dependent manner (*34*). This is required for correct spindle assembly and chromosome segregation during mitosis. The methylation at the N-terminus of H2B may have additional functions that are unknown.

Differentiation of trimethylation from acetylation is essential in PTM studies of histones (*13*). A typical method for distinguishing these two modifications is based on the immonium ion at *m*/*z* 126.1 from acetylated lysine and the neutral loss of a trimethylamine [$N(CH_3)_3$] from trimethyllysine-containing precursor and fragment ions (*13*). However, the method does not work effectively with peptides containing more than one acetylation or trimethylation site, such as the H2B N-terminal peptide, which includes multiple modified lysines. In our study, we were able to differentiate these two modifications on the basis of subtle differences in mass increase of the lysine residue induced by acetylation and trimethylation. For instance, the measured mass difference between the b_6 and b_7 ions observed in Figure 2C for the peptide segment including residues 1−12 was 832.5055−662.3982 = 170.1073 Da. This mass difference is closer to that expected for K7 acetylation (170.1056 Da, with a relative deviation of 9.9 ppm) than that expected for trimethylation of K7 (170.1420 Da, with a relative deviation of 204 ppm). We therefore concluded that K7 is acetylated. All the acetylation and trimethylation sites of *Neurospora* core histones were unambiguously established in this way, and more sample results are listed in Table S1 of the Supporting Information.

The presence of an acetylated lysine can block trypsin cleavage of its C-terminal side amide bond. With many lysine residues being acetylated, tryptic cleavage of H2B gives rise to a very long N-terminal peptide. Traditional collisionally induced dissociation (CID) cannot provide a complete series of fragment ions because of its poor ability to cleave the backbone of large peptides, rendering it difficult to identify modification sites. For instance, the exact numbers of methyl groups on the N-terminus and K3 cannot be delineated unambiguously on the basis of the CID-produced MS/MS on the tetramethylated peptide with residues 1−12 (Figure 2C). To overcome this limitation, we applied ETD, which can afford efficient cleavage along the backbone of long peptides or even intact proteins (*35*, *36*), to analyze those large N-terminal peptides. Figure 3 shows the ETD MS/MS of the $[M + 5H]^{5+}$ ion of peptide $_1$PPKPADKKPASKAPATASKAPEKK$_{24}$, with the N-terminus and K3 being dimethylated and K7, K12, and K19 being acetylated. Nearly complete series of c and z ions were formed from ETD. The observation of c_2 + 2Me and c_4 + 4Me ions reveals the dimethylation of the N-terminus and K3. The presence of the c_6 + 4Me, c_7 + 4Me + Ac, z_{17} + 2Ac, and z_{18} + 3Ac ions supported the K7 acetylation, while the existence of the c_{11} + 4Me + Ac, c_{12} + 4Me + 2Ac, z_{12} + Ac, and z_{13} + 2Ac ions demonstrated the K12 acetylation. Along this line, the acetylation of K19 was identified on the basis of the observation of the z_5 and z_6 + Ac ions. K28 and K29 were also found to be acetylated heterogeneously in *Neurospora* H2B, as supported by the coexistence of y_5, y_5 + Ac, b_4, and b_4 + Ac ions in the MS/MS of the Asp-N-produced peptide $_{25}$DAGKKTAASG$_{34}$ (Figure S4A of the Supporting Information).

Purified H2A was digested individually with trypsin, Arg-C, or chymotrypsin under optimized conditions and analyzed by LC−MS/MS. We found that only K9 was acetylated (MS/MS for the $[M + 2H]^{2+}$ ion of $_6$SGGKASGSKNAQSR$_{19}$ shown in

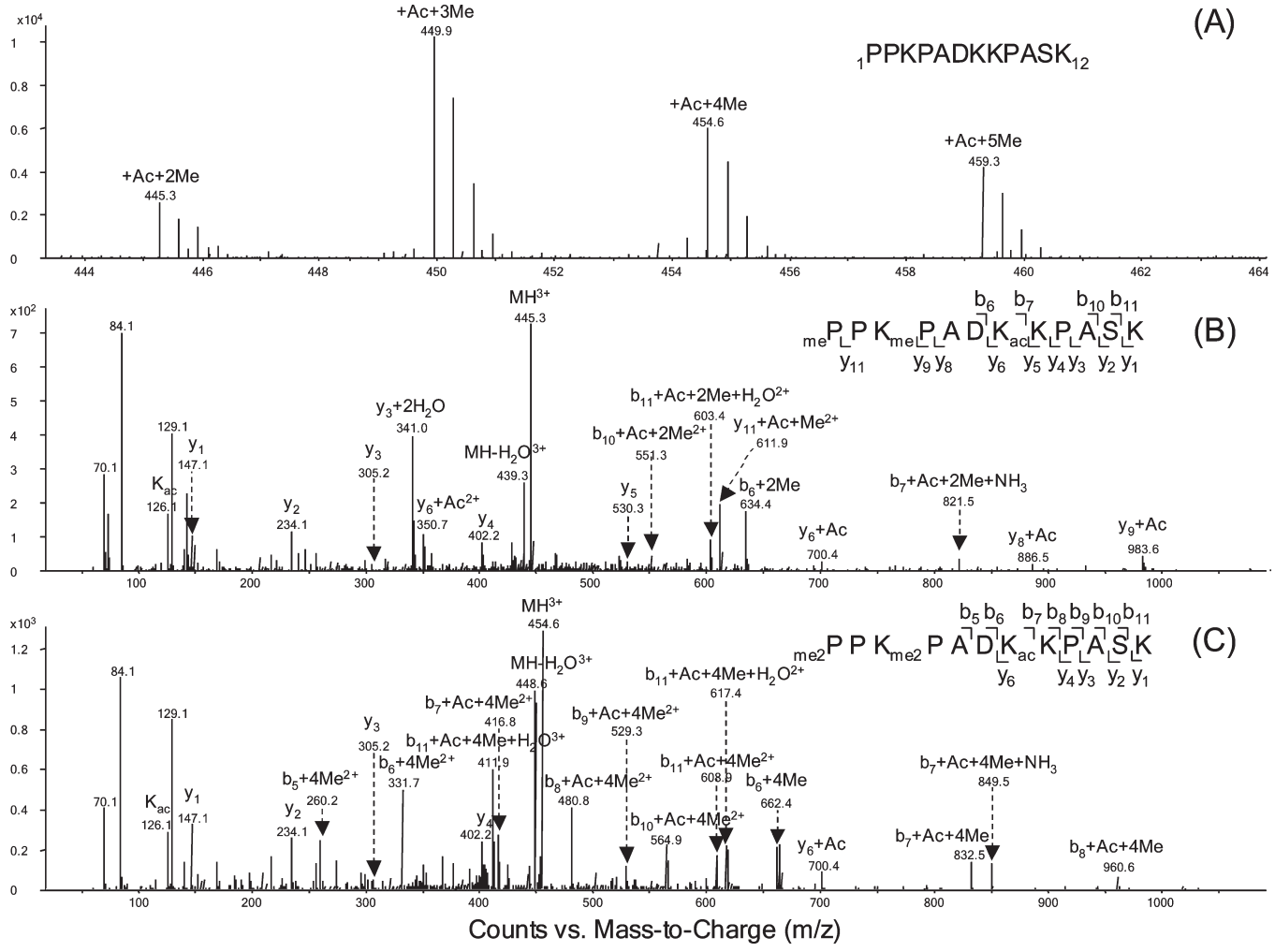

FIGURE 2: (A) ESI-MS of N-terminal tryptic peptide $_1$PPKPADKKPASK$_{12}$ of histone H2B extracted from *Neurospora*. (B and C) MS/MS of the dimethylated, monoacetylated (B) and tetramethylated, monoacetylated (C) H2B peptide with residues 1−12 obtained by Q-TOF analysis.

Figure S4B of the Supporting Information, which reveals the formation of the b_4 + Ac, y_{10}, and y_{11} + Ac ions).

Identification of PTMs in Histone H3. HPLC-purified histone H3 was digested with Arg-C and Glu-C, and the digestion mixture was analyzed by LC−MS/MS directly, or further fractionated by HPLC and analyzed by MALDI-MS/MS. All the conserved methylation and acetylation sites reported in other organisms were identified in *Neurospora*, including methylation at K4, K9, K27, K36, and K79 and acetylation at K9, K14, K18, K23, K27, and K56. K4 was found to be mono-, di-, and trimethylated, whereas K79 was found to be mono- and dimethylated in *Neurospora* (Figure S5A,B of the Supporting Information). In the MS/MS of the $[M + 2H]^{2+}$ ion (m/z 366.7) of trimethylated peptide $_3$TKQTAR$_8$ (Figure S5C), we observed the b_3 + 3Me, b_4 + 3Me, and y_4 ions, supporting the observed trimethylation of K4. The MS/MS of dimethylated peptide segment $_{73}$EIAQDFKSDLR$_{83}$ displayed the presence of a complete series of y ions, revealing dimethylation of K79 (Figure S5D). Figure S5E illustrates the fragmentation of the precursor ion at m/z 646.9, which is consistent with the acetylation of K56 in peptide $_{54}$YQKSTELLIR$_{63}$. In the MS/MS of triply charged peptide $_9$KSTGGKAPRKQLASKAAR$_{26}$, K9, K14, K18, and K23 were shown to be acetylated (Figure S5F), with the observation of the b_2 + Ac ion for supporting K9 acetylation, the b_5 + Ac and b_7 + 2Ac ions for K14 acetylation, and y_1, y_5 + Ac, and y_{11} + 2Ac ions for K18 and K23 acetylation.

It is worth noting that K9 and K27 were found to be either methylated or acetylated. The methylated and acetylated peptides exhibited different retention times on the reverse-phase column used for LC−MS/MS analysis; the retention times for the methylated and acetylated peptides with residues 9−17 were approximately 4 and 8 min, respectively (Figure S6 of the Supporting Information). Thus, methylated and acetylated peptides could be well isolated, and unambiguous MS/MS could be obtained. Figure 4A shows the ESI-MS of the triply charged ions of the unmodified, mono-, di-, and trimethylated peptides with residues $_9$KSTGGKAPR$_{17}$, while Figure 4B shows the MS for the acetylated peptide with the same sequence. In the MS/MS of the $[M + 3H]^{3+}$ ions of the trimethylated and acetylated peptides, a series of trimethylated and acetylated b ions and unmodified y ions were observed, supporting the conclusion that K9 was trimethylated and acetylated, respectively (Figure 4C,D). The presence of the immonium ion at m/z 126, the neutral loss of $N(CH_3)_3$ (59 Da) from the precursor ion, and the mass difference between trimethylation and acetylation helped differentiate these two types of isobaric modifications.

K27 was also found to be mono-, di-, or trimethylated or acetylated in *Neurospora* (Figure S7A,B of the Supporting Information). The MS/MS of peptide $_{27}$KSAPSTGGVKKPHR$_{42}$ with

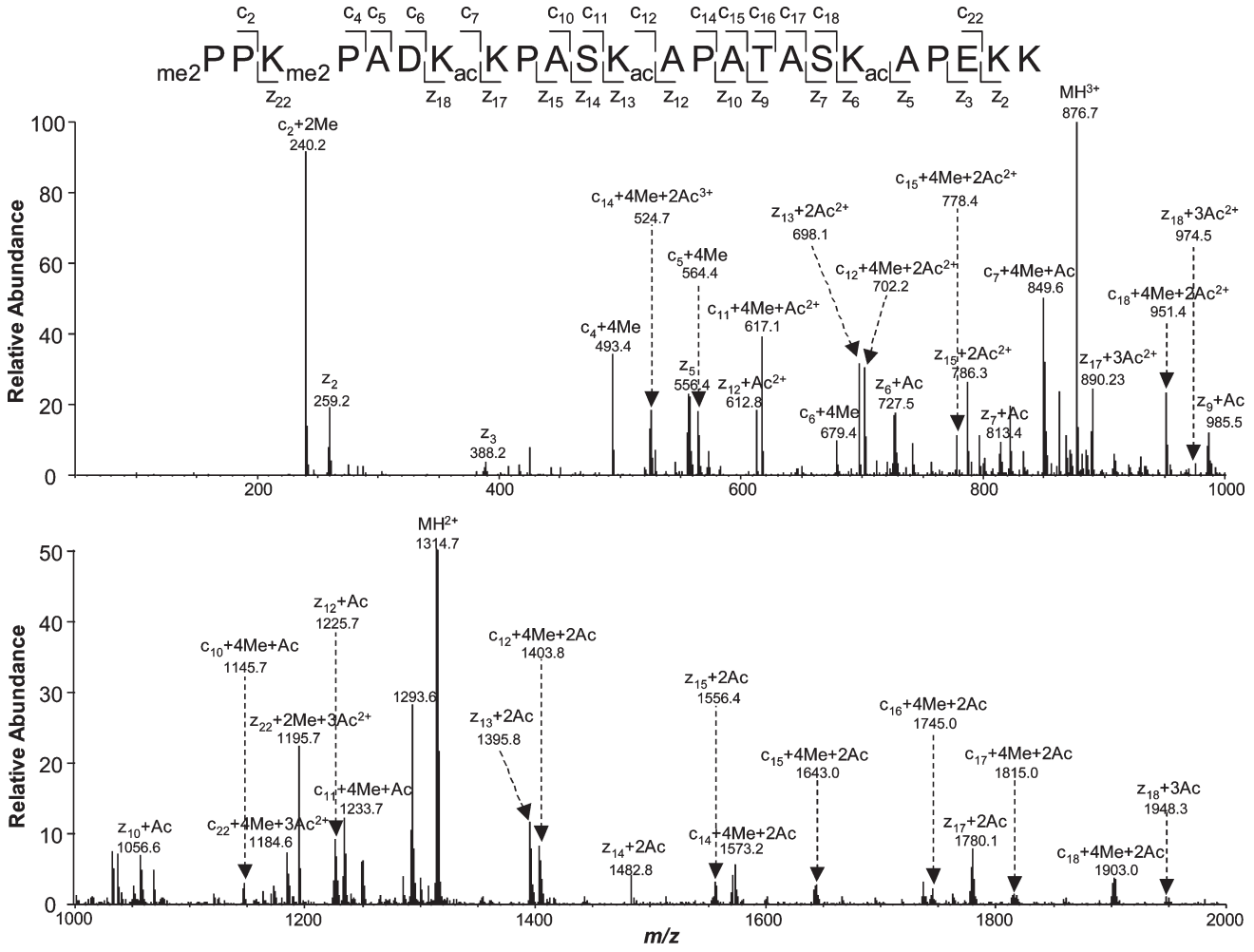

FIGURE 3: ETD MS/MS of the *Neurospora* H2B N-terminal peptide, with residues 1−24 with the N-terminus and K3 being dimethylated and K7, K12, and K19 being acetylated.

different modification levels were obtained via selected ion monitoring. The MS/MS of the $[M + 4H]^{4+}$ ion at m/z 384.2 eluted at 16 and 18 min revealed the trimethylation on K36 as well as the trimethylation or acetylation on K27. In this context, the presence of the $y_7 + 3me$, $y_8 + 3me$, $y_9 + 3me$, $y_{10} + 3me$, and $y_{11} + 3me$, along with the observation of the y_1, y_2, and y_4 ions, demonstrates the trimethylation on K36 (Figure S7C,D). On the other hand, the acetylation and trimethylation on K27 are manifested by the presence of b_2 and b_3 ions bearing an acetyl group and three methyl groups, respectively (Figure S7C,D).

We also attempted to examine the phosphorylation of core histones by enriching phosphorylated peptides using TiO_2-coated magnetic beads [phosphopeptide enrichment kit (PerkinElmer, Waltham, MA)] (*37*). We were able to detect a very low level of phosphorylation of H3 S10 in a phosphatase-deficient (PP1-deficient) *Neurospora* strain (Figure S8 of the Supporting Information) (*20*); H3 S10 phosphorylation in wild-type *Neurospora* was, however, below the detection limit of the instruments.

Identification of PTMs in Histone H4. Purified H4 was digested by trypsin and Asp-N separately and subjected to LC− or MALDI-MS/MS analysis. All the modifications were located on the N-terminal segment, similar to observations for other organisms. Asp-N digestion produced a long N-terminal peptide with residues $_1$TGRGKGGKGLGKGGAKRHRKILR$_{23}$, containing all the modification sites in H4, which include acetylation at the N-terminus and at K5, K8, K12, and K16, along with methylation at K20 (Figure S9A of the Supporting Information). A LTQ-Orbitrap with ETD provided high-quality tandem mass spectra of the $[M + 6H]^{6+}$ ions of the peptide with a nearly complete series of c and z ions. Figure S9B shows an ETD MS/MS of the diacetylated and trimethylated peptide with residues 1−23. The formation of the monoacetylated small c ions and $z_{20} + 3Me + Ac$ ions suggests N-terminal acetylation. Additionally, the presence of $c_{15} + Ac$, $c_{16} + 2Ac$, $z_7 + 3Me$, and $z_8 + 3Me + Ac$ ions and $c_{19} + 2Ac$, $c_{20} + 2Ac + 3Me$, z_3, and $z_4 + 3Me$ ions supports the conclusions of K16 acetylation and K20 trimethylation, respectively.

LC−MS/MS analysis, with the use of the QTOF mass spectrometer, of the tryptic digestion mixture led to the identification of relatively low levels of acetylation on K5, K8, and K12, which cannot be identified from the corresponding analyses of the Asp-N digestion mixture of histone H4. In the MS/MS of doubly charged peptide $_4$GKGGKGLGK$_{12}$, K5 and K8 were determined to be acetylated, as exemplified by the observations of the $b_2 + Ac$, $b_5 + 2Ac$, y_4, $y_5 + Ac$, and $y_7 + Ac$ ions (Figure S10A of the Supporting Information). MS/MS of the doubly charged ion of diacetylated peptide $_9$GLGKGGAKR$_{17}$ revealed the formation of b_3, $b_4 + Ac$, $y_5 + Ac$, and $y_6 + 2Ac$ ions supporting the K12 acetylation, and the presence of the y_1 and $y_2 + Ac$ ions demonstrates the acetylation of K16 (Figure S10B).

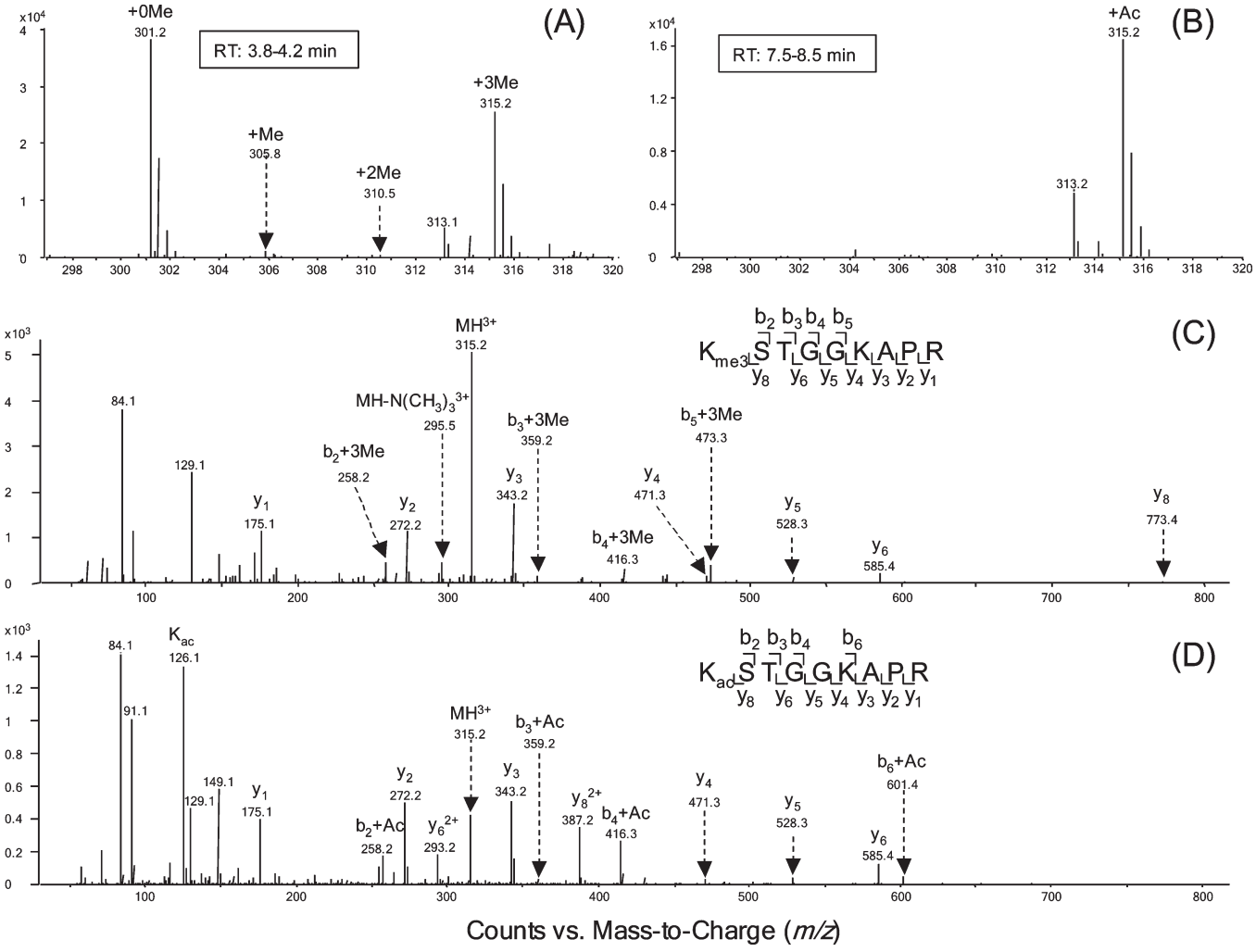

FIGURE 4: Positive-ion ESI-MS of the Arg-C-produced *Neurospora* H3 peptide $_{9}$KSTGGKAPR$_{17}$ with K9 being methylated (A) or acetylated (B). Shown in panels C and D are the MS/MS, obtained for the Q-TOF mass spectrometer, of the trimethylated and acetylated peptides with residues 9−17.

Table 1: Comparison of Core Histone Methylation and Acetylation among Different Organisms, Including *N. crassa*, *S. cerevisiae*, *A. thaliana*, and *H. sapiens* (*14*, *26*, *38*, *39*)

		modification sites			
histone	modification	*N. crassa*	*S. cerevisiae*	*A. thaliana*	*H. sapiens*
H2B	methylation	N-terminus, K3			
	acetylation	K7, K12, K19, K28, K29	K3, K6, K11, K16, K21, K22	K6, K11, K27, K32	K5, K11, K12, K15, K16, K23
H2A	acetylation	K9	K4, K7	K5, K144	K5, K9
H3	methylation	K4, K9, K27, K36, K79	K4, K36, K79	K4, K9, K27, K36	K4, K9, K27, K36, K79
	acetylation	K9, K14, K18, K23, K27, K56	K9, K14, K18, K23, K27, K56	K9, K14, K18, K23	K9, K14, K18, K23, K27
H4	methylation	K20	K20		K20
	acetylation	N-terminus, K5, K8, K12, K16	N-terminus, K5, K8, K12, K16	K5, K8, K12, K16	N-terminus, K5, K8, K12, K16

DISCUSSION

We used a combination of various mass spectrometric methods, including MALDI-TOF and LC−MS/MS with CID and ETD, coupled with different protease digestions and HPLC purification, to produce a thorough map of lysine methylation and acetylation sites in the core histones of the filamentous fungus *N. crassa*. Our results show that the core histones in this organism are extensively acetylated and/or methylated on the lysine residues that have been found acetylated and/or methylated in mammals, budding yeast, and plants. In addition, some novel modifications were detected. *Neurospora* H2B undergoes N-terminal and K3 methylation and K7, K12, K19, K28, and K29 acetylation. Some of these sites, along with additional sites in the globular and C-terminal domain of the protein, were also found to be modified in the following study (DOI 10.1021/bi100391w), where the histone proteins were fractionated with two-dimensional AUT × AU polyacrylamide gels containing acetic acid, urea, and Triton X-100 prior to the mass spectrometric study. H2A was shown to be acetylated at K9. H3 was found to be methylated at K4, K9, K27, K36, and K79 and to be subject to acetylation at K9, K14, K18, K23, K27, and K56. Finally, H4 was found to be methylated at K20 and acetylation at the N-terminus,

K5, K8, K12, and K16 (summarized in Figure 1). In this context, it is worth noting that some low levels of modification in *Neurospora* might not have been detected even with the combination of multiple protease digestions and various mass spectrometric techniques. A detailed comparison of known PTMs of core histones in different organisms is summarized in Table 1 (*14*, *26*, *38*, *39*). The N-terminal and K3 methylation that we observed in H2B appears to be novel. H2A was found to be acetylated only at K9 in *Neurospora*, as in humans. As noted in Table 1, we found conserved acetylation of H2B at K7 and K12 (the corresponding residues in other organisms are K6 and K11, respectively), and unique acetylation of *Neurospora* H2B at K19, K28, and K29. It has been reported that acetylated lysine residues in yeast H2B activate the transcription of genes involved in NAD biosynthesis and vitamin metabolism (*40*). Thus, it will be interesting to assess the role of *Neurospora* H2B acetylation in transcription activation. Indeed, a detailed comparison of histone H2B from a histone deacetylase mutant and wild-type *Neurospora* revealed differences that might be responsible for defects in DNA methylation observed in this mutant (K. M. Smith, J. R. Dobosy, D. Do, J. E. Riefsnyder, D. C. Anderson, G. R. Green, and E. U. Selker, manuscript preparation) (DOI 10.1021/bi100391w).

In *Neurospora* H3, we found all the commonly conserved N-terminal modifications, including methylation of K4, K9, K27, and K36 and acetylation of K9, K14, K18, K23, and K27. K4 was mostly unmodified, but approximately 10% of the K4 peptide was mono-, di-, or trimethylated. K9 was predominantly trimethylated. K27 and K36 were mono-, di-, and trimethylated. The methylated and acetylated peptides housing the same residues had different retention times during HPLC separation, allowing the modification types to be easily determined. Moreover, we observed acetylation at K56. The predominant form of H3 K9 methylation observed in our data, trimethylation, was previously shown to be enriched in regions of DNA methylation in the *Neurospora* genome (*41*, *42*). The SET domain methyltransferase DIM-5 catalyzes this modification and is required for DNA methylation (*43*). Unlike in plants and mammals, in *Neurospora* H3 K36 mono-, di-, and trimethylation is catalyzed by a single enzyme, SET-2 (*21*). H3 K36 methylation is enriched in coding regions of the genome and is required for normal vegetative and sexual development (*21*).

H3K79 is mono-, di-, or trimethylated in many mammalian and nonmammalian cell lines and in budding yeast. However, K79 was found only mono- and dimethylated in *Neurospora*. It would be interesting to explore the functional implications of the lack of K79 trimethylation, since the H3 K79 methyltransferase, DOT1, is involved in telomeric silencing in yeast (*44*). In addition, it is worth noting that K64 of H3 of mammalian cells was recently found to be trimethylated; this methylation is associated with heterochromatin, and it is lost during developmental reprogramming (*45*). We monitored specifically the fragmentation of the peptide containing this putative modification by MS/MS but did not find this modification in *Neurospora*. It is possible that the level of this modification is below the detection limits of the method; conceivably, it could also have been lost during the extraction process.

Histone H4 acetylation sites, including the N-terminus, and residues K5, K8, K12, and K16, are conserved in almost all organisms, including *Neurospora*. They play important roles in many processes, including transcriptional activation, DNA double-strand break repair, and cellular lifespan regulation (*46*, *47*). H4 K20 methylation, conserved in almost all multicellular organisms, was also found in *Neurospora*, in the form of mono-, di-, and mainly trimethylation. While its role in heterochromatin silencing and DNA damage response has been extensively studied in humans, *Drosophila melanogaster*, and *Schizosaccharomyces pombe* (*48*−*51*), it is also important to study its function in *Neurospora*.

In summary, a systematic mapping of histone methylation and acetylation in *N. crassa* was obtained by mass spectrometric analyses. The rigorous identification of modification sites provides a foundation for further studies of the regulation and functions of histone modifications in this model organism.

ACKNOWLEDGMENT

We thank Dr. Lihua Jiang at Thermo for performing the ETD experiments and Dr. David C. Anderson for communicating his findings prior to publication.

SUPPORTING INFORMATION AVAILABLE

HPLC trace for the fractionation of core histones and LC−MS/MS results. This material is available free of charge via the Internet at http://pubs.acs.org.

REFERENCES

1. McGhee, J. D., and Felsenfeld, G. (1980) Nucleosome structure. *Annu. Rev. Biochem. 49*, 1115–1156.
2. Luger, K., Mader, A. W., Richmond, R. K., Sargent, D. F., and Richmond, T. J. (1997) Crystal structure of the nucleosome core particle at 2.8 Å resolution. *Nature 389*, 251–260.
3. Strahl, B. D., and Allis, C. D. (2000) The language of covalent histone modifications. *Nature 403*, 41–45.
4. Berger, S. L. (2002) Histone modifications in transcriptional regulation. *Curr. Opin. Genet. Dev. 12*, 142–148.
5. Geiman, T. M., and Robertson, K. D. (2002) Chromatin remodeling, histone modifications, and DNA methylation: How does it all fit together? *J. Cell. Biochem. 87*, 117–125.
6. Nacheva, G. A., Guschin, D. Y., Preobrazhenskaya, O. V., Karpov, V. L., Ebralidse, K. K., and Mirzabekov, A. D. (1989) Change in the pattern of histone binding to DNA upon transcriptional activation. *Cell 58*, 27–36.
7. Irvine, R. A., Lin, I. G., and Hsieh, C. L. (2002) DNA methylation has a local effect on transcription and histone acetylation. *Mol. Cell. Biol. 22*, 6689–6696.
8. Peterson, C. L., and Laniel, M. A. (2004) Histones and histone modifications. *Curr. Biol. 14*, R546–R551.
9. Cheung, P., Allis, C. D., and Sassone-Corsi, P. (2000) Signaling to chromatin through histone modifications. *Cell 103*, 263–271.
10. Jenuwein, T., and Allis, C. D. (2001) Translating the histone code. *Science 293*, 1074–1080.
11. Klose, R. J., and Zhang, Y. (2007) Regulation of histone methylation by demethylimination and demethylation. *Nat. Rev. Mol. Cell Biol. 8*, 307–318.
12. Fillingham, J., and Greenblatt, J. F. (2008) A histone code for chromatin assembly. *Cell 134*, 206–208.
13. Zhang, K., Yau, P. M., Chandrasekhar, B., New, R., Kondrat, R., Imai, B. S., and Bradbury, M. E. (2004) Differentiation between peptides containing acetylated or tri-methylated lysines by mass spectrometry: An application for determining lysine 9 acetylation and methylation of histone H3. *Proteomics 4*, 1–10.
14. Beck, H. C., Nielsen, E. C., Matthiesen, R., Jensen, L. H., Sehested, M., Finn, P., Grauslund, M., Hansen, A. M., and Jensen, O. N. (2006) Quantitative proteomic analysis of post-translational modifications of human histones. *Mol. Cell. Proteomics 5*, 1314–1325.
15. Bernstein, B. E., Humphrey, E. L., Erlich, R. L., Schneider, R., Bouman, P., Liu, J. S., Kouzarides, T., and Schreiber, S. L. (2002) Methylation of histone H3 Lys 4 in coding regions of active genes. *Proc. Natl. Acad. Sci. U.S.A. 99*, 8695–8700.
16. Kurdistani, S. K., Tavazoie, S., and Grunstein, M. (2004) Mapping global histone acetylation patterns to gene expression. *Cell 117*, 721–733.
17. Ng, H. H., Robert, F., Young, R. A., and Struhl, K. (2003) Targeted recruitment of Set1 histone methylase by elongating Pol II provides a

localized mark and memory of recent transcriptional activity. *Mol. Cell 11*, 709–719.
18. Galagan, J. E., Calvo, S. E., Borkovich, K. A., Selker, E. U., Read, N. D., Jaffe, D., FitzHugh, W., Ma, L. J., Smirnov, S., Purcell, S., Rehman, B., Elkins, T., Engels, R., Wang, S., Nielsen, C. B., Butler, J., Endrizzi, M., Qui, D., Ianakiev, P., Bell-Pedersen, D., Nelson, M. A., Werner-Washburne, M., Selitrennikoff, C. P., Kinsey, J. A., Braun, E. L., Zelter, A., Schulte, U., Kothe, G. O., Jedd, G., Mewes, W., Staben, C., Marcotte, E., Greenberg, D., Roy, A., Foley, K., Naylor, J., Stange-Thomann, N., Barrett, R., Gnerre, S., Kamal, M., Kamvysselis, M., Mauceli, E., Bielke, C., Rudd, S., Frishman, D., Krystofova, S., Rasmussen, C., Metzenberg, R. L., Perkins, D. D., Kroken, S., Cogoni, C., Macino, G., Catcheside, D., Li, W., Pratt, R. J., Osmani, S. A., DeSouza, C. P., Glass, L., Orbach, M. J., Berglund, J. A., Voelker, R., Yarden, O., Plamann, M., Seiler, S., Dunlap, J., Radford, A., Aramayo, R., Natvig, D. O., Alex, L. A., Mannhaupt, G., Ebbole, D. J., Freitag, M., Paulsen, I., Sachs, M. S., Lander, E. S., Nusbaum, C., and Birren, B. (2003) The genome sequence of the filamentous fungus *Neurospora crassa*. *Nature 422*, 859–868.
19. Davis, R. H., and Perkins, D. D. (2002) Timeline: *Neurospora*: A model of model microbes. *Nat. Rev. Genet. 3*, 397–403.
20. Adhvaryu, K. K., and Selker, E. U. (2008) Protein phosphatase PP1 is required for normal DNA methylation in *Neurospora*. *Genes Dev. 22*, 3391–3396.
21. Adhvaryu, K. K., Morris, S. A., Strahl, B. D., and Selker, E. U. (2005) Methylation of histone H3 lysine 36 is required for normal development in *Neurospora crassa*. *Eukaryotic Cell 4*, 1455–1464.
22. Selker, E. U., Fritz, D. Y., and Singer, M. J. (1993) Dense nonsymmetrical DNA methylation resulting from repeat-induced point mutation in *Neurospora*. *Science 262*, 1724–1728.
23. Emmett, N., Williams, C. M., Frederick, L., and Williams, L. S. (1972) Arginyl-transfer ribonucleic acid and synthetase of *Neurospora crassa*. *Mycologia 64*, 499–509.
24. Goff, C. G. (1976) Histones of *Neurospora crassa*. *J. Biol. Chem. 251*, 4131–4138.
25. Xiong, L., Ping, L., Yuan, B., and Wang, Y. (2009) Methyl group migration during the fragmentation of singly charged ions of trimethyllysine-containing peptides: Precaution of using MS/MS of singly charged ions for interrogating peptide methylation. *J. Am. Soc. Mass Spectrom. 20*, 1172–1181.
26. Zhang, K., Sridhar, V. V., Zhu, J., Kapoor, A., and Zhu, J. K. (2007) Distinctive core histone post-translational modification patterns in *Arabidopsis thaliana*. *PLoS One 2*, e1210.
27. Zhang, K. L. (2008) Characterization of acetylation of *Saccharomyces cerevisiae* H2B by mass spectrometry. *Int. J. Mass Spectrom. 278*, 89–94.
28. Clayton, A. L., Hebbes, T. R., Thorne, A. W., and Cranerobinson, C. (1993) Histone Acetylation and Gene Induction in Human Cells. *FEBS Lett. 336*, 23–26.
29. Grimes, S. R., and Henderson, N. (1984) Acetylation of rat testis histones H2B and Th2B. *Dev. Biol. 101*, 516–521.
30. Desrosiers, R., and Tanguay, R. M. (1988) Methylation of *Drosophila* histones at proline, lysine, and arginine residues during heat shock. *J. Biol. Chem. 263*, 4686–4692.
31. Martinage, A., Briand, G., Van Dorsselaer, A., Turner, C. H., and Sautiere, P. (1985) Primary structure of histone H2B from gonads of the starfish *Asterias rubens*. Identification of an N-dimethylproline residue at the amino-terminal. *Eur. J. Biochem. 147*, 351–359.
32. Nomoto, M., Kyogoku, Y., and Iwai, K. (1982) N-Trimethylalanine, a novel blocked N-terminal residue of *Tetrahymena* histone H2B. *J. Biochem. 92*, 1675–1678.
33. Bergmuller, E., Gehrig, P. M., and Gruissem, W. (2007) Characterization of post-translational modifications of histone H2B-variants isolated from *Arabidopsis thaliana*. *J. Proteome Res. 6*, 3655–3668.
34. Chen, T., Muratore, T. L., Schaner-Tooley, C. E., Shabanowitz, J., Hunt, D. F., and Macara, I. G. (2007) N-terminal α-methylation of RCC1 is necessary for stable chromatin association and normal mitosis. *Nat. Cell Biol. 9*, 596–603.
35. Syka, J. E., Coon, J. J., Schroeder, M. J., Shabanowitz, J., and Hunt, D. F. (2004) Peptide and protein sequence analysis by electron transfer dissociation mass spectrometry. *Proc. Natl. Acad. Sci. U.S.A. 101*, 9528–9533.
36. Mikesh, L. M., Ueberheide, B., Chi, A., Coon, J. J., Syka, J. E., Shabanowitz, J., and Hunt, D. F. (2006) The utility of ETD mass spectrometry in proteomic analysis. *Biochim. Biophys. Acta 1764*, 1811–1822.
37. Larsen, M. R., Thingholm, T. E., Jensen, O. N., Roepstorff, P., and Jorgensen, T. J. (2005) Highly selective enrichment of phosphorylated peptides from peptide mixtures using titanium dioxide microcolumns. *Mol. Cell. Proteomics 4*, 873–886.
38. Garcia, B. A., Hake, S. B., Diaz, R. L., Kauer, M., Morris, S. A., Recht, J., Shabanowitz, J., Mishra, N., Strahl, B. D., Allis, C. D., and Hunt, D. F. (2007) Organismal differences in post-translational modifications in histones H3 and H4. *J. Biol. Chem. 282*, 7641–7655.
39. Sinha, I., Wiren, M., and Ekwall, K. (2006) Genome-wide patterns of histone modifications in fission yeast. *Chromosome Res. 14*, 95–105.
40. Parra, M. A., Kerr, D., Fahy, D., Pouchnik, D. J., and Wyrick, J. J. (2006) Deciphering the roles of the histone H2B N-terminal domain in genome-wide transcription. *Mol. Cell. Biol. 26*, 3842–3852.
41. Tamaru, H., Zhang, X., McMillen, D., Singh, P. B., Nakayama, J., Grewal, S. I., Allis, C. D., Cheng, X., and Selker, E. U. (2003) Trimethylated lysine 9 of histone H3 is a mark for DNA methylation in *Neurospora crassa*. *Nat. Genet. 34*, 75–79.
42. Lewis, Z. A., Honda, S., Khlafallah, T. K., Jeffress, J. K., Freitag, M., Mohn, F., Schubeler, D., and Selker, E. U. (2009) Relics of repeat-induced point mutation direct heterochromatin formation in *Neurospora crassa*. *Genome Res. 19*, 427–437.
43. Tamaru, H., and Selker, E. U. (2001) A histone H3 methyltransferase controls DNA methylation in *Neurospora crassa*. *Nature 414*, 277–283.
44. Ng, H. H., Feng, Q., Wang, H. B., Erdjument-Bromage, H., Tempst, P., Zhang, Y., and Struhl, K. (2002) Lysine methylation within the globular domain of histone H3 by Dot1 is important for telomeric silencing and Sir protein association. *Genes Dev. 16*, 1518–1527.
45. Daujat, S., Weiss, T., Mohn, F., Lange, U. C., Ziegler-Birling, C., Zeissler, U., Lappe, M., Schubeler, D., Torres-Padilla, M. E., and Schneider, R. (2009) H3K64 trimethylation marks heterochromatin and is dynamically remodeled during developmental reprogramming. *Nat. Struct. Mol. Biol. 16*, 777–781.
46. Dang, W., Steffen, K. K., Perry, R., Dorsey, J. A., Johnson, F. B., Shilatifard, A., Kaeberlein, M., Kennedy, B. K., and Berger, S. L. (2009) Histone H4 lysine 16 acetylation regulates cellular lifespan. *Nature 459*, 802–807.
47. Bird, A. W., Yu, D. Y., Pray-Grant, M. G., Qiu, Q., Harmon, K. E., Megee, P. C., Grant, P. A., Smith, M. M., and Christman, M. F. (2002) Acetylation of histone H4 by Esa1 is required for DNA double-strand break repair. *Nature 419*, 411–415.
48. Fang, J., Feng, Q., Ketel, C. S., Wang, H. B., Cao, R., Xia, L., Erdjument-Bromage, H., Tempst, P., Simon, J. A., and Zhang, Y. (2002) Purification and functional characterization of SET8, a nucleosomal histone H4-lysine 20-specific methyltransferase. *Curr. Biol. 12*, 1086–1099.
49. Rice, J. C., Nishioka, K., Sarma, K., Steward, R., Reinberg, D., and Allis, C. D. (2002) Mitotic-specific methylation of histone H4 Lys 20 follows increased PR-Set7 expression and its localization to mitotic chromosomes. *Genes Dev. 16*, 2225–2230.
50. Sanders, S. L., Portoso, M., Mata, J., Bahler, J., Allshire, R. C., and Kouzarides, T. (2004) Methylation of histone H4 lysine 20 controls recruitment of Crb2 to sites of DNA damage. *Cell 119*, 603–614.
51. Schotta, G., Lachner, M., Sarma, K., Ebert, A., Sengupta, R., Reuter, G., Reinberg, D., and Jenuwein, T. (2004) A silencing pathway to induce H3-K9 and H4-K20 trimethylation at constitutive heterochromatin. *Genes Dev. 18*, 1251–1262.